Project Number 282910

ÉCLAIRE

Effects of Climate Change on Air Pollution Impacts and Response Strategies for European Ecosystems

Seventh Framework Programme

Theme: Environment

D5.3 Quantifying the importance of long-range transport for ecosystem impacts- final report.

Due date of deliverable: **01/10/2014**

Actual submission date: **11/03/2015**

Start Date of Project: **01/10/2011**

Duration: **48 months**

Organisation name of lead contractor for this deliverable :
European Commission, Joint Research Centre

Project co-funded by the European Commission within the Seventh Framework Programme		
Dissemination Level		
PU	Public	x
PP	Restricted to other programme participants (including the Commission Services)	☐
RE	Restricted to a group specified by the consortium (including the Commission Services)	☐
CO	Confidential, only for members of the consortium (including the Commission Services)	☐

1. Executive Summary

While deposition and ozone have been reported in 5.1 and 5.4, in this deliverable report the focus is to provide updated and reliable BVOC and wildfire emissions estimate at global and European scale for present and future scenarios.

We present in D5.3 results from two different biogenic VOC (BVOC) emission models (ORCHIDEE and LPJ) on European and global scale. LPJ results also provided information on changes in fire related emissions.

Results can be summarized as follows (see main text):

- In Europe, comparison of biogenic VOC emissions calculated with the widely used MEGAN emission model and the vegetation model ORCHIDEE, showed 19% higher isoprene emissions, 21% higher methanol and 21% lower monoterpene emissions by the latter. Assumptions on leaf-temperature for shaded and sunlit leaves versus air temperature play an important role in explaining these differences. Assumptions on leaf-area-index (LAI) also are a major uncertainty, with a complex impact on emission variability.
- Globally, comparing the 2040s and the 1990s, Orchidee calculations indicate 25% increase in isoprene, 27% in monoterpenes and 28% in methanol emissions. However, isoprene emission potential may decrease caused by higher levels of CO2, resulting in complete off-setting of isoprene emissions.
- LPJ-GUESS calculations of BVOC emission in Europe indicate a decline of isoprene and monoterpene emissions by about a factor of 3 comparing the landcover in 2000s to the potential natural vegetation. Simulations are highly sensitive to biases in climate models- leading to ca. 65 % and 20 % lower emissions for isoprene and monoterpene emissions compared to using bias-corrected emissions.
- LPJ-GUESS calculations of BVOC global emissions the RCP4.5 GHG scenario, indicate isoprene emissions increase 41% and monoterpenes 25% in the future compared to current conditions. However, taking the CO_2 inhibition effect into account, emissions decrease slightly with -2% and -13% respectively for isoprene and monoterpenes. Climate change favors isoprene emitting vegetation.
- LPJ-GUESS calculations of wildfire emissions indicate a complex range of interactions between vegetation, climate change and increasing CO2, and fire suppression. Comparing 1970-2000 and 2070-2100, overall tropical emissions decline between 15 and 35 % (mostly due human influence), while extratropical emissions increase by 20 % and 45 %. Globally emissions change within a -10 % range.
- While nitrogen input to ecosystems affects yields and can lead to pollution of water sheds in heavily fertilised regions, effects of N deposition on natural ecosystems regarding the historical carbon sink strength are minor. Whether or not nitrogen limitation of plant growth will notably affect future ecosystem carbon storage is under debate, and current modelling studies show conflicting results. Arguably, climate effects of N_2O emissions are of more concern than N-interactions with the C sink; this will be investigated further in the coming years with updated versions of LPJ-GUESS.

2. Objectives

The objectives of D5.3 were to analyze the evolution of key environmental variables impacting ecosystems (ozone levels, PM levels, N and S deposition) under the various emission and climate scenarios and isolate the role played by long-range transport of pollution, climate change and changing variability, biogenic/emissions, lightning emissions, and anthropogenic emissions in Europe and other regions.

3. Activities:

We report two activities regarding biogenic and wildfire emission under present and future conditions with two different vegetation models.

3.1 The CNRS/LSCE group (Palmira Messina, Juliette Lathière, Didier Hauglustaine) updated the biogenic VOC emission module (Lathière et al., 2006) in the global vegetation model ORCHIDEE (Organizing Carbon and Hydrology in Dynamic EcosystEms). Specifically (see also D6.2), we ORCHIDEE was updated:

i. adding new emitted compounds
ii. re-examining all the Emission Factors (EFs) considering state of the art emission schemes and the most recent

field measurements

iii. adding a light dependency for almost all emitted species as already carried out for isoprene
iv. activating the leaf age emission correction factor
v. activating and adapting the multi-layer radiation scheme

We present here the fixed version of the biogenic emission module that includes two more developments:

vi. improvements of the multi-layer radiation scheme
vii. inclusion of CO2 inhibition for isoprene emissions

The multi-layer radiation scheme in ORCHIDEE is based on Spitter et al. (1986a,b), with the light profile within the canopy determined by the amount of light at the top of the canopy and by the extinction coefficient of the different radiation components. The light follows an exponential decrease with Leaf Area Index (LAI) when going deeper into the canopy. In the model the LAI is divided in up to 17 levels, with the number of levels depending on the LAI value. For each layer, the percentage of sunlit and shaded leaves besides together with the diffuse and direct component of the solar radiation are calculated.

The inhibition effect of increasing atmospheric CO2 concentrations on isoprene emissions is now quantified in the model. Two different approaches can be activated, (i) the first one is based on Possell et al. (2005) where one correction factor, depending only on atmospheric CO2 concentration, is applied to every Plant Functional Type (PFT); (ii) the second one is based on Wilkinson et al., (2009) where the correction factor depends on both the atmospheric and the intercellular CO2 concentrations and therefore varies among PFTs.

3.2 The University of Lund group (Almut Arneth, Wolfgang Knorr, Stijn Hantson, Michao Wu) updated the LPJ_GUESS model to evaluate change in biogenic and wildfire emissions from the 21st century.
Specific update were made regarding the coupled CN cycle, revised vegetation representation, accounting for human land-cover changes), as previously described in deliverable D3.4.

Natural vegetation emissions of ozone and aerosol precursors under present-day and future conditions have been calculated with the dynamic vegetation model LPJ-GUESS [*Smith et al.*, 2001; *Smith et al.*, 2014]. The model simulates changes in emissions of the biogenic volatile organic compounds (BVOC) isoprene and monoterpenes [*Arneth et al.*, 2008a; *Arneth et al.*, 2007; *Schurgers et al.*, 2009a]. BVOC emissions respond directly to changes in air temperature and radiation levels, as well as to changes in vegetation productivity (especially changes in the emitting leaf area) and changes in vegetation species composition. The latter has been shown to have a large effect, since different vegetation types have very different emission capacities resulting in large emission changes in response to anthropogenic land-cover changes [*Rosenkranz et al.*, 2014]. BVOC emissions also respond to levels of CO_2 in the atmosphere – indirectly, due to vegetation growth-response. The model is also designed to assess the direct inhibition of leaf-level emission, which has been shown to affect emissions of isoprene, even though the effects on monoterpenes are unknown [*Arneth et al.*, 2008b; *Niinemets et al.*, 2010]. Latest updates made to the modelling framework as part of the Eclaire project (e.g., coupled CN cycle, revised vegetation representation, accounting for human land-cover changes) have been described in deliverable D3.4.
Wildfire emissions in LPJ-GUESS depend on burned area, and the amount and type of combusted plant material. Following Knorr et al. [*Knorr et al.*, 2014], burned area is calculated in response to changes in climate (e.g., warmer temperatures affecting fire risk), changes in CO_2 concentration (e.g., affecting vegetation and fuel type, and vegetation and fuel structure – both important for fire spread), and changes in population numbers and rural *vs*. urban population structure (both measures for effects of changing land use on wildfire, as well as subsumed human effects related to ignitions and extinctions). Emissions are then computed applying emission factors for various vegetation types and chemical species [*Andreae and Merlet*, 2001; *Knorr et al.*, 2012].
BVOC and wildfire emissions have been calculated from present-day to the end of the 21st century using climate change projections from different historical (e.g., CRU) and future projections from general circulation models (e.g., IPSL, CCSM and MPI-ESM), using a range of CO_2 emission, population and land-use change scenarios.

4. Results:

4.1 Modeling with the ORCHIDEE and MEGAN models

BVOC emissions estimated by ORCHIDEE are extensively compared to those obtained by the MEGAN model (Guenther et al., 2012). The two models are run at the global scale for a period of 10 years (2000 to 2009) with a resolution of 0.5° x 0.5°. Regarding the ORCHIDEE model, it was necessary to perform a spin-up of 20 years in order to equilibrate the leaf stock/compartment. Both MEGAN and ORCHIDEE are forced with the same climate based on the CRU-NCEP re-analysis. Unlike ORCHIDEE, the MEGAN model does not compute the leaf-area-index (LAI). Therefore, in the results presented here, the ORCHIDEE simulation provided the LAI used in MEGAN.

In Table 5.3.1 we show the global emission budget averaged along the simulation period (2000-2009). In general the two models show a very good agreement. MEGAN emission estimates are 19% higher for isoprene, 21% higher for methanol and 21% lower for monoterpenes, compared to ORCHIDEE. The largest differences (more than 50%) are found for sesquiterpenes and α-Pinene. Regarding other species, the absolute difference is between 10-24%.

Compounds	ORCHIDEE	MEGAN
Isoprene	353.9	422.7
Methanol	34.0	41.1
Acetone	24.3	20.2
Acetaldhyde	7.7	8.5
Formaldhyde	1.67	1.55
Acetic Acid	1.00	1.16
Formic Acid	0.65	0.76
MBO	1.34	1.08
Sesqiterpenes	23.1	14.5
Monoterpenes	89.9	74.0
α-Pinene	38.6	24.5
β-Pinene	11.5	13.0

Table 5.3.1. Mean global emission budget in TgC/year calculated by ORCHIDEE and MEGAN over the 2000-2009 period.

The spatial pattern of annual emissions (Figure 5.3.1 and 5.3.2) presents several differences between the two models. Emissions calculated for tropical trees are generally higher in ORCHIDEE compared to MEGAN (for example for monoterpenes, alpha pinene, beta pinene, acetone, in Brazil, Equatorial Africa and Indonesia) while considering other PFTs, even in the tropical area, MEGAN emissions are usually higher. This discrepancy is due to the fact that in ORCHIDEE the air temperature is used to calculate emissions while MEGAN considers the leaf temperature. Indeed in the case of leaf shade in dense vegetation area, the leaf temperature can be significantly lower than the air temperature, leading to lower emissions. Large differences in term of spatial distribution and amounts are underlined for isoprene emissions, especially in Brazil. This behavior is principally driven by the different EF pattern between MEGAN and ORCHIDEE.

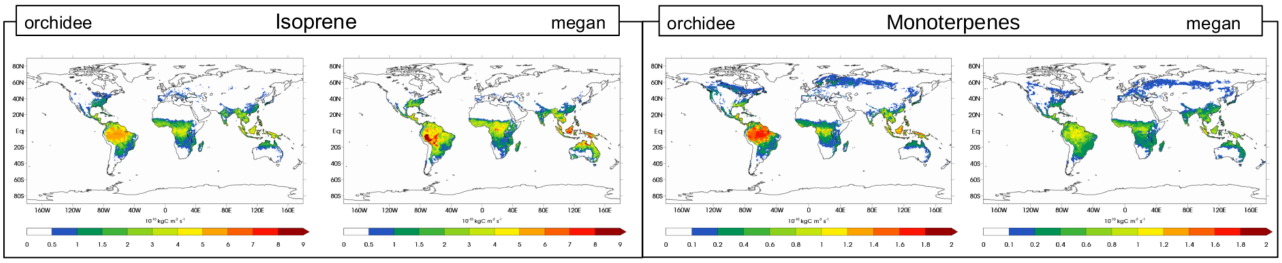

(a)

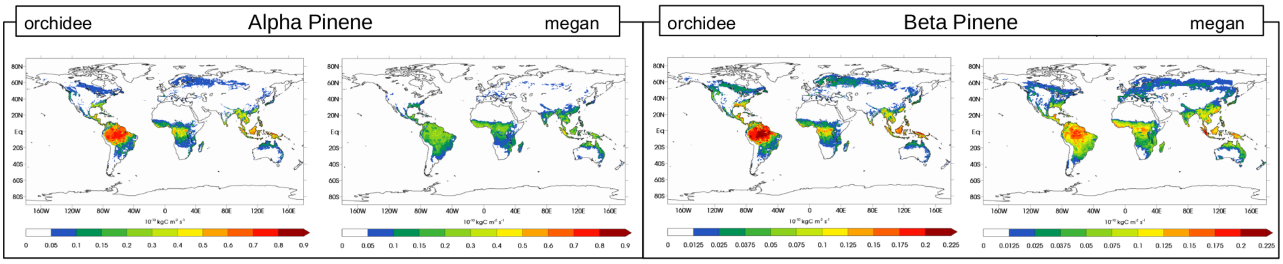

(b)

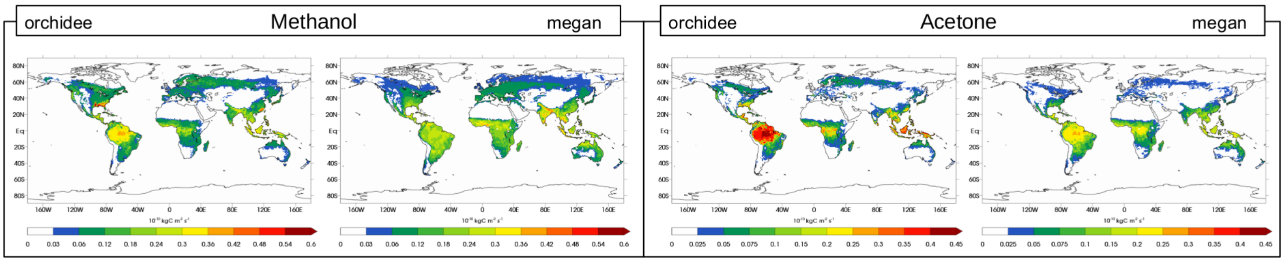

(c)

Figure 5.3.1. Annual emissions averaged over 2000-2009 (10^{10}kgC/m^2/s) for ORCHIDEE and MEGAN.

The monthly variations of emissions for different regions (tropics, temperate and boreal) are shown in Figure 5.3.2. Seasonal trends are very similar between the two models especially for the temperate and boreal region, where we observe a good agreement even in the range of estimates. More differences occur in tropical regions, where we observe that ORCHIDEE calculated higher emissions for alpha-pinene, monoterpenes and acetone compared to MEGAN, and lower emissions for isoprene, methanol and beta-pinene.

(a)

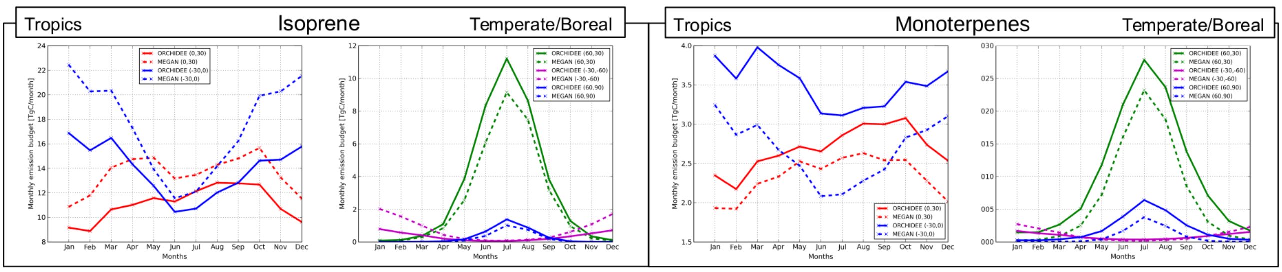

(b)

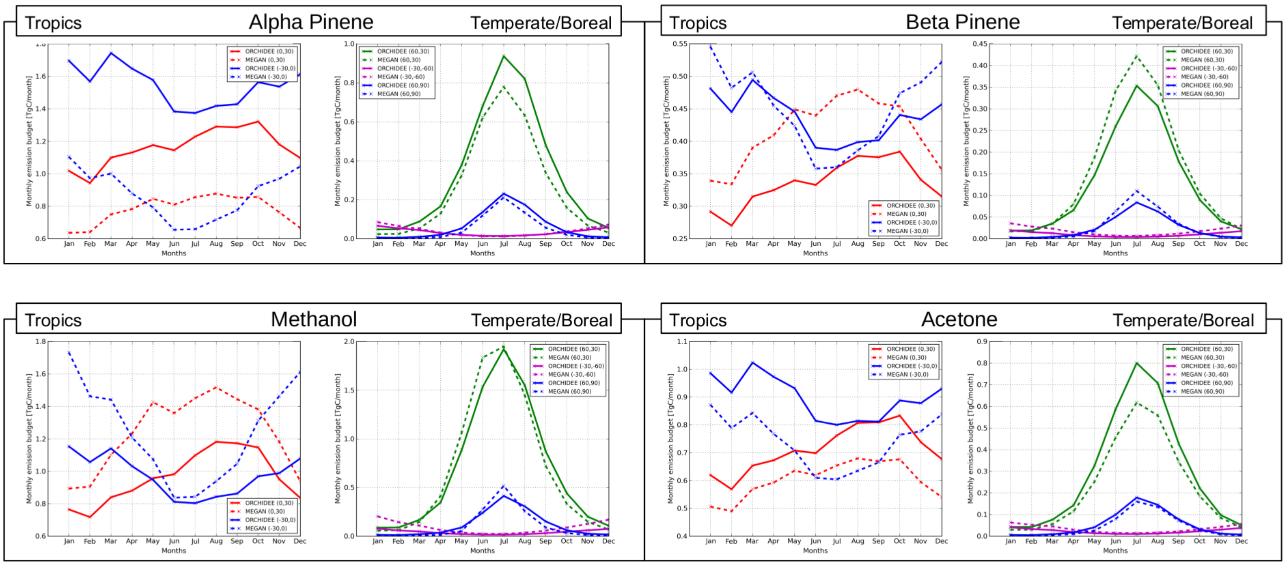

(c)

Figure 5.3.2. Zonal average of the emissions for ORCHIDEE (solid lines) and MEGAN (dashed lines) for different biogenic compounds during 2000-2009. In each couple of figures the left one represents the zonal average for North (0°, 30°) (red lines) and South tropics (-30°, 0°) (blue lines) and the right one the zonal average for North temperate area (30°, 60°) (green lines), South temperate (-30°, 60°) (purple lines) and North boreal region (60°, 90°)(blue lines). Emissions are expressed in TgC/month.

ORCHIDEE and MEGAN sensitivity to LAI

LAI was identified as one of the major uncertainties in biogenic emission modeling. Therefore, in this section we investigate the BVOC emission sensitivity to LAI variation in ORCHIDEE and MEGAN model. LAI can be modeled, as done in ORCHIDEE, retrieved by satellite or directly measured. However estimates from measurements and models can be significantly different, and there is therefore still a non-negligible uncertainty in LAI values, regional and temporal variability (Garrigues et al., 2008, Pinty et al., 2012, Fang et al., 2012). In Figure 5.3.3 we present, as an example, the comparison between the LAI calculated by ORCHIDEE (solid black line) and that one retrieved by MODIS (red line) (Yuan et al., 2011). MODIS LAI retrievals were recently used to estimate BVOC emissions with MEGAN in the framework of MACC II project (Sindelarova et al., 2014). As shown in figure 5.3.3 the difference between both LAI is close to a factor of two. It is therefore important to better quantify the range of uncertainty in BVOCs emission linked to the LAI uncertainty.

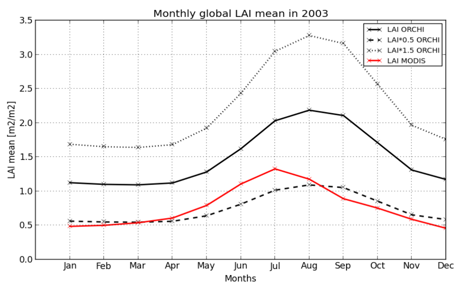

Figure 5.3.3. Global monthly mean LAI calculated by ORCHIDEE (solid black line) and retrieved from MODIS measurements (red line). The dashed lines represent the LAI by ORCHIDEE multiplied by a factor 0.5 (thick dashed line) and 1.5 (thin dashed line).

Sensitivity tests, varying the LAI (LAI*0.5 and LAI*1.5), are performed using the ORCHIDEE and MEGAN models. In this case the simulation period is limited to the year 2003. In the Figure 5.3.4 the zonal average in the North temperate region (30°N– 60°N) and the North tropical region (0°N – 30°N) are depicted for isoprene and monoterpenes emissions, respectively. Considering isoprene emissions we observe that ORCHIDEE and MEGAN present a similar response to LAI variations, between -13% and 3% for MEGAN and between -13% and 5% for ORCHIDEE while the behavior of monoterpenes is rather different. ORCHIDEE is more sensitive to LAI change (between -44% and 41%) compared to MEGAN (between -10% and 2.5%).

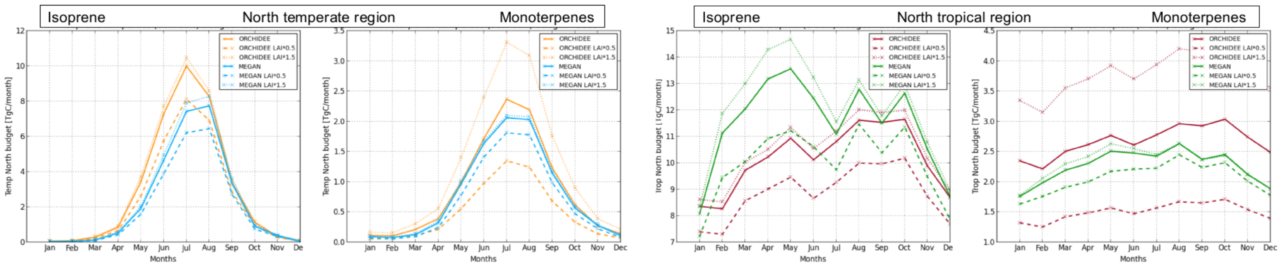

Figure 5.3.4. Zonal average of emissions in the different sensitivity tests (LAI not varied in solid line, LAI*0.5 in thin dashed line and LAI*0.5 in thick dashed line) during 2003 and related to the North temperate region (first couple of figures, starting from the left) and the North tropical region (second couple of figures). In each couple of figures the left one represents isoprene and the right one monoterpenes. Emissions are expressed in TgC/month.

The differences observed are linked to the non-light dependent part of the emissions that, for monoterpenes, represents the 40% of the total emissions. In ORCHIDEE the air temperature is used to calculate emissions, while in MEGAN the leaf temperature is considered. This implies that in MEGAN biogenic compounds are mostly emitted by sunlit leaves, while in ORCHIDEE both sunlit and shade leaves contribute equally to biogenic emissions. Multiplying LAI by 2, for instance, does not necessarily imply doubling the amount of sunny leaves. Indeed the partition between shaded and sunny leaves is not linear and could even bring to a slight decrease in sunlit leaves in locations where vegetation is dense, in relation with leaf self-shading effect. The emissions that are principally drive by sunlit leaves therefore do not necessarily increase, when LAI increases. Similar consideration can be done in the case of dividing LAI by 2.
In order to better investigate the role of leaf and air temperatures in the emission sensitivity, we are implementing a module for the calculation of the leaf temperature, following the approach used in the MEGAN model (Guenther et al., 2012), which is not part of the work reported here.

Key message:
In Europe, comparison of biogenic VOC emissions calculated with the widely used MEGAN emission model and the vegetation model ORCHIDEE, showed 19% higher isoprene emissions, 21% higher methanol and 21% lower monoterpene emissions by the latter. Assumptions on leaf-temperature for shaded and sunlit leaves versus air temperature play an important role in explaining these differences. Assumptions on leaf-area-index (LAI) also are a major uncertainty, with a complex impact on emission variability.

Future BVOC emissions at European scale
We provide, using the update version of the ORCHIDEE BVOC emission module, the emissions at European scale for present and future scenarios. A present-day simulations (from 1990 to 2000) and a future scenario (from 2040 to 2050) are performed. A spin up of 20 years is preformed, to equilibrate the LAI, for both simulations. We use as climatic forcing files the 3-hourly database adapted for ORCHIDEE and based on the RCA3 European down-scaling of the ECHAM5 A1B-r3 simulation (Kjellstrom et al. 2011; provided by M. Engardt in the framework of the ECLAIRE project). The vegetation distribution is based on Land-Use scenarios corresponding to the RCP 8.5 and is kept constant using the year 2000.

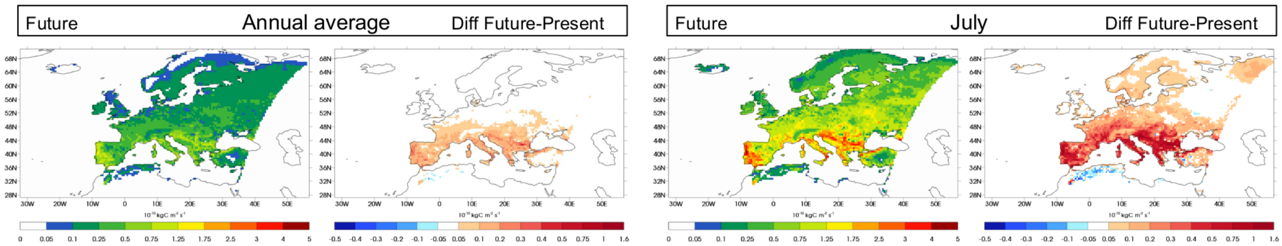

(a) Isoprene

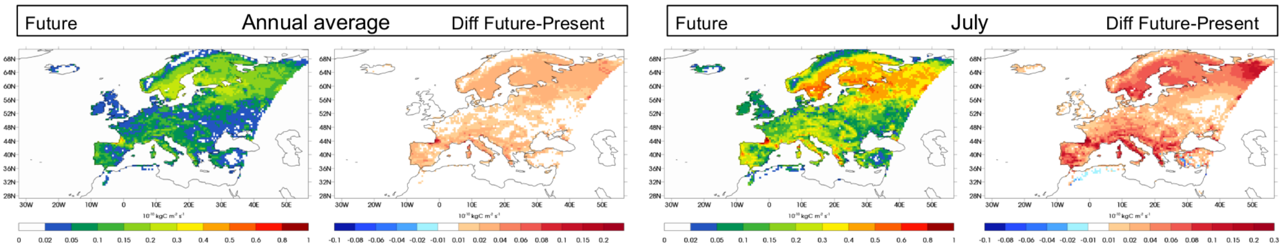

(b) Monoterpene

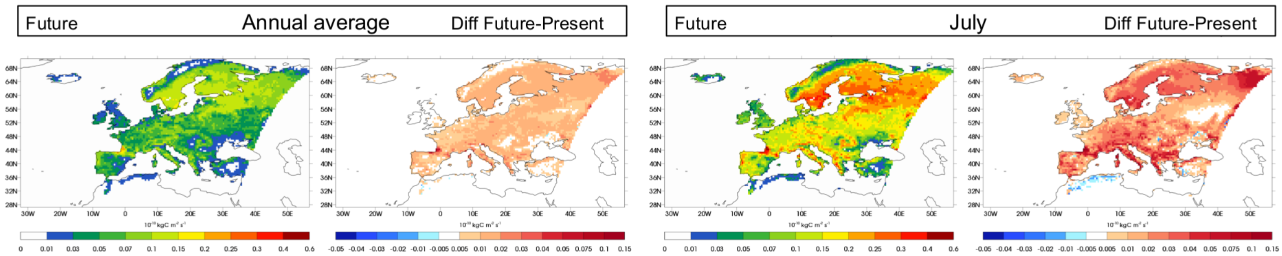

(c) Methanol
(d) Acetone

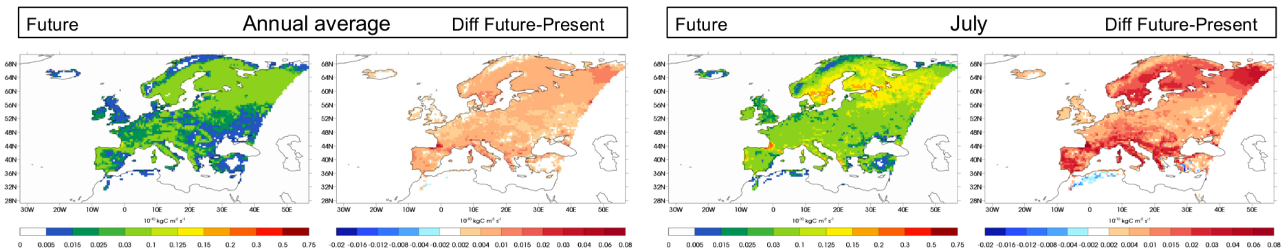

Figure 5.3.5. European emissions of (a) isoprene, (b) monoterpene, (c) methanol and (d) acetone. From left-to-right the first panel represents the annual average for the future scenario; the 2nd panel the difference between the annual average of the future scenarios and the present; the third and fourth panel are the same to the previous ones, but related to the month of July. Emissions are given in 10^{10}kgC/m^2/s.

In the future scenario, we observe (figure 5.3.5) a general increase of BVOC emissions for whole Europe, in particular in June, July and August. With respect to the present scenarios, the future increase reaches 20% for isoprene, 17% for moneterpene and acetone and 16% for methanol emissions.

It is worth to underline that these simulations are not following the ECLAIRE protocol stated in the WP6, but can be considered as a test for the new forcing climate data and a first quantification of the BVOC emissions change in Europe in the future. Further simulations following the WP6 protocol are planned for the coming months.

Key Message:
Globally, comparing the 2040s and the 1990s, Orchidee calculations indicate 25% increase in isoprene, 27% in monoterpenes and 28% in methanol emissions. However, isoprene emission potential may decrease caused by higher levels of CO2, resulting in complete off-setting of isoprene emissions.

Future BVOC emission scenarios at global scale
Present (1990s) and future (2050s) BVOC emission scenarios are performed and evaluated at the global scale. These simulations used a coarser resolution of 2.5° x 3.75°, the A1B climate forcing scenario and the vegetation distribution based on the RCP 8.5. Forcings used are therefore consistent with the WP6 protocol for European simulations. Different simulations are performed in order to isolate and compare the effects of future change in climate, land-use and CO2 (inhibition effect on isoprene) on BVOC emission change. Regarding the CO2 inhibition effect on isoprene either the approach based on Possell et al. 2005 or Wilkinson et al. 2009 is activated for intercomparison. For 2050s global annual emissions are estimated to increase by 25% for isoprene, 27% for monoterpenes and 28% for methanol, compared to 1990s emissions. When the CO2 inhibition effect is considered, as described by Wilkinson et al. (2009), a decrease by 9% is calculated for global annual isoprene emissions compared to the present-day scenario, therefore completely counteracting the effect of future change in climate.

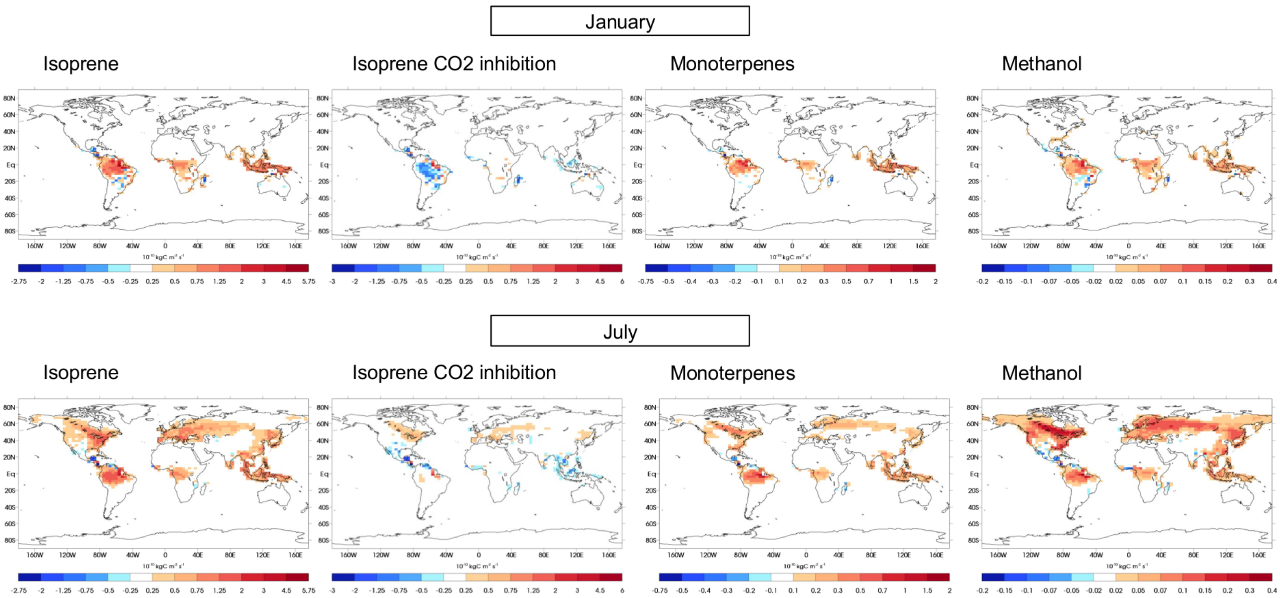

Figure 5.3.6. Difference between the future and present scenario for January (first line) and July (second line). In each line the first figure is related to isoprene, the second one to isoprene activating the CO2 inhibition (Wilkinson method) and the third and forth figures to monoterpens and methanol.

Key Message: Globally, comparing the 2040s and the 1990s, Orchidee calculations indicate a 25% increase in isoprene, 27% in monoterpenes and 28% in methanol emissions. However inclusion of in case of isoprene increased stomata closure by higher levels of CO2 may result complete offsetting of isoprene emissions.

4.2 Emission modeling using the LPJ-GUESS model

4.2.1 Vegetation BVOC Emissions in Europe
Simulations of isoprene and monoterpene emission across Europe, with the latest Eclaire-version of LPJ-GUESS are consistent with previously published work [*Arneth et al.*, 2008a; *Schurgers et al.*, 2009b] in that the relatively largest source for isoprene is in the central to southern parts of Europe. For monoterpene emissions, a strong source is also located in southern Europe, but overall, emissions are much more evenly spread over the entire continent (Figure 5.3.8;

see also D3.4). As has been discussed before [*Arneth et al.*, 2008a; *Schurgers et al.*, 2009b] these spatial patterns reflect a complex mix of weather patterns affecting emissions (e.g., warm temperatures and high light fostering production and emissions of both isoprene and monoterpenes), combined with species composition (e.g., species with high monoterpene basal emission rates being abundant across Europe). Including the CN-coupling, in the latest version of LPJ-GUESS did not change these previously modelled spatial patterns greatly (Figure 5.3.8).

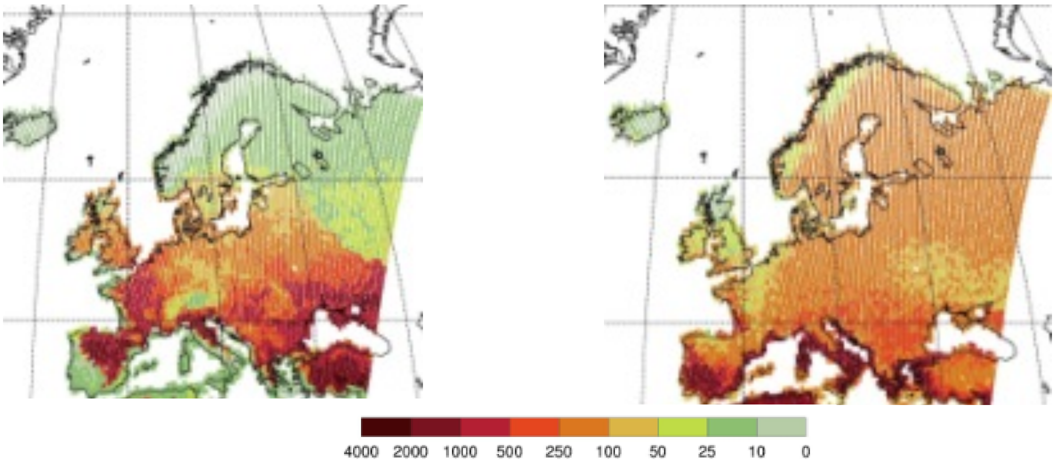

Figure 5.3.8. Present-day (1971-2000) isoprene (left) and monoterpene (right) emissions (in mgC m^{-2} a^{-1}) from potential vegetation (not accounting for land use changes). Simulations were done with MPI-ESM climate, bias-corrected to CRU (data from [Ahlstrom et al., 2012]).

In the latest version of LPJ-GUESS, human agricultural activities and land-cover changes are taken into consideration [*Lindeskog et al.*, 2013]. Human land-cover changes -affected both isoprene and monoterpene emissions in Europe over the entire 20th century, typically reducing emissions, especially so for isoprene to around one third [*Rosenkranz et al.*, 2014]. For monoterpenes (using same historical climate) changes were much smaller, and included areas of increase as well as decrease in emissions (Figure 5.3.9, Table 5.3.2). The overriding cause of these differences lies in the assigned emission potentials of vegetation: for isoprene, the crops replacing (mostly) woody natural vegetation have much lower emission potentials, whereas regarding monoterpenes (Figure 5.3.9 left) emissions, some crops have emissions quite comparable to the natural vegetation they replace [*Kesselmeier and Staudt*, 1999; *Rosenkranz et al.*, 2014].

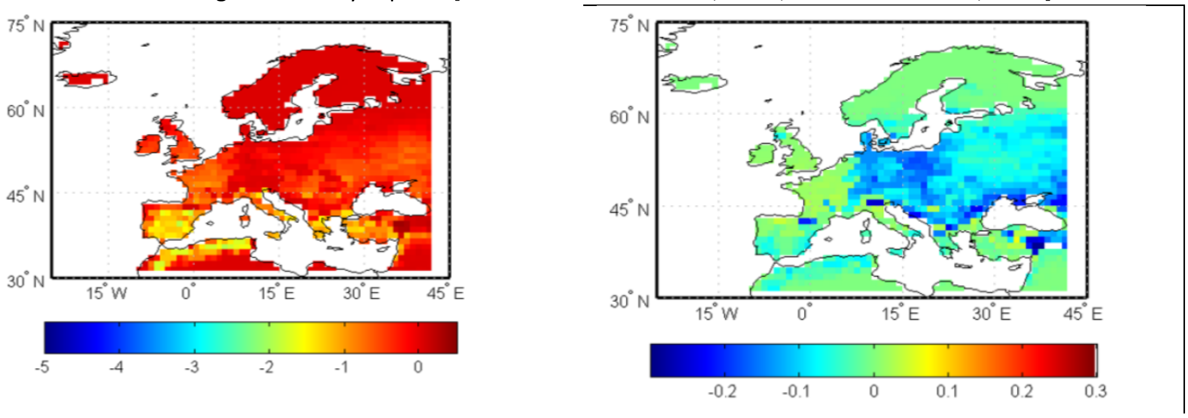

Figure 5.3.9. Effect of human land cover changes for present-day climate (1971-2000) isoprene (left) and monoterpene (right) emissions (in gC m^{-2} a^{-1}). Simulations were done with MPI-ESM climate, bias-corrected to CRU (data from [Ahlstrom et al., 2012]).

Differences in climate drivers affect emissions notably, pointing to a large source of uncertainty, both for historical, but also for future projections. Both land-cover change and climate change thus need to be accounted for, including variability in their projections, when simulating BVOC emissions and their effect on air quality. For instance, taking non-bias corrected climate from a regional climate model (example: SMHI) reduced emissions of isoprene and monoterpene emissions notably below values simulated with the observation-based historical climate from University of East Anglia

(CRU; Table 5.3.2). Most likely this is due to much lower levels of radiation in the non-bias corrected RCM climate, which is also reflected in the much lower values of net primary productivity.

Table 5.3.2. Simulated averaged annual European isoprene and monoterpene (AMON) emissions, as well as vegetation net (ANPP) primary productivity. Numbers are for historical gridded climate from CRU, compared with non-bias corrected regional climate model output (SMHI), for potential natural vegetation, and 2000 human land cover change.

ISOPRENE (mgC/m2/a)		1981-2002	2041-2050
	SMHI	216	194
	CRU	361	n.a.
	SMHI-N-LC2000	84	71
MONOTERPENE (mgC/m2/a)	SMHI	245	203
	CRU	295	n.a.
	SMHI-N-LC2000	83	73
ANPP (kgC/m2/a)	SMHI	0.32	0.33
	CRU	0.46	n.a.
	SMHI-N-LC2000	0.28	0.34

Key message: LPJ-GUESS calculations of BVOC emission in Europe indicate a decline of isoprene and monoterpene emissions by about a factor of 3 comparing the landcover in 2000s to the potential natural vegetation. Simulations are highly sensitive to biases in climate models- leading to ca. 65 % and 20 % lower emissions for isoprene and monoterpene emissions compared to using bias-corrected emissions.

4.2.2 Global vegetation emissions

As shown before in a number of BVOC emission simulation studies (for review see eg., [*Arneth et al.*, 2008b; *Arneth et al.*, 2011]), the Eclaire simulations with LPJ-GUESS have by far the highest isoprene emission source in tropical regions (Figure 5.3.10), related to warm, sunny weather conditions, large emitting leaf area, and large emission capacities. By contrast, large emission sources for monoterpenes can not only be found in the tropics, but also in large areas of the warm temperate biomes (Figure 5.3.10; [*Hantson et al.*, 2015]).

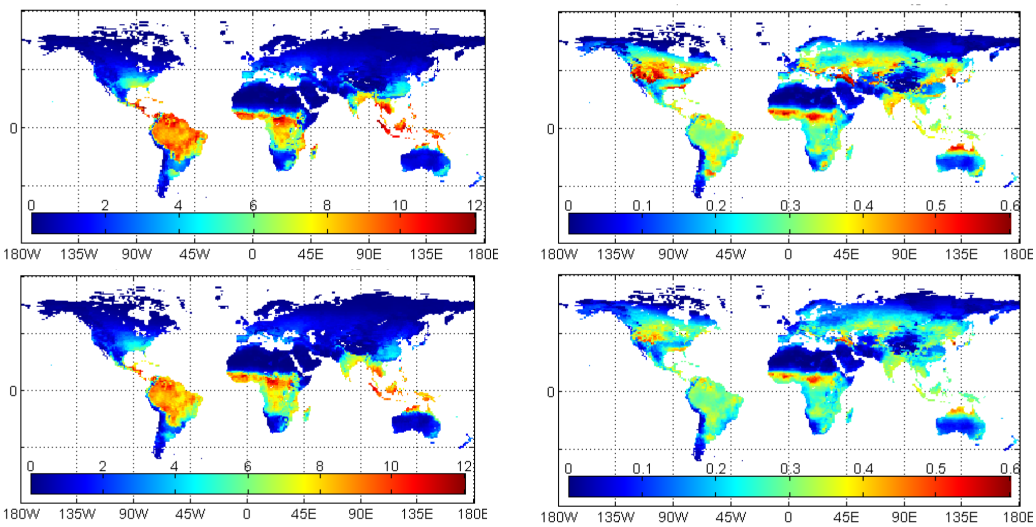

Figure 5.3.10. Present (top: 1981-2000) and future (bottom: 2081-2100) emissions in gC/yr/m2 for Isoprene (left) and monoterprenes (right). Simulations are with MPI-ESM climate model output with RCP 4.5 emissions, and CO_2 inhibition switched on. From Hantson et al. (in preparation).

At global scale, emissions of isoprene for the late 20th century are reduced by approximately 10% in response to anthropogenic land cover changes [*Arneth et al.*, 2008b], mainly when forested areas are transformed into crops and pastures, since crop and pasture vegetation has much lower emission capacities. By contrast, monoterpene emissions, globally, are affected only to small degree by converting natural vegetation into agriculture, since also crop species tend to have relatively large monoterpene emission capacities [*Kesselmeier and Staudt*, 1999].

Table 5.3.3. Mean annual BVOC emissions for natural vegetation using MPI-ESM future (2080-2100) climate with the RCP4.5 GHG and land-use scenario, with and without CO2 inhibition. Land use change is not taken into account.

Period	CO2 inhibition	Isoprene (TgC/yr)	Monoterpenes (TgC/yr)
1981-2000	-	385	28.6
2081-2100	*On*	377	24.8
2081-2100	*Off*	544	35.7

The spatial emission patterns remain largely the same under future climate condition (example shown in Figure 5.3.10). The absolute numbers, however, are strongly determined by the uncertainty in the CO_2 inhibition effect. When the CO_2 inhibition of leaf emissions is ignored, both isoprene and monoterpene emissions increase strongly under future conditions. For the RCP4.5 GHG scenario, isoprene emissions increase 41% and monoterpenes 25% in the future compared to current conditions (Table 5.3.3). However, when we take into account the CO_2 inhibition effect, emissions decrease slightly with -2% and -13% respectively for isoprene and monoterpenes (Table 5.3.3).

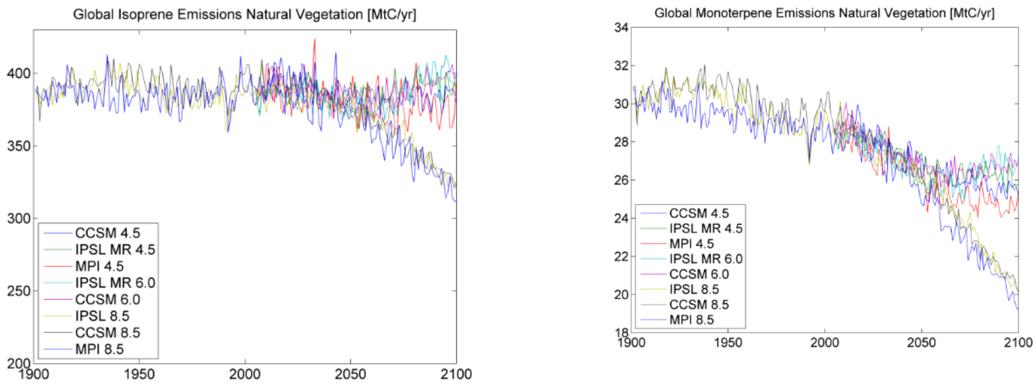

Figure 5.3.11. Isoprene (left) and monoterpene (right) emissions for potential natural vegetation. Simulations were performed for a set of different GCMs, and emissions scenarios, having CO2 inhibition switched on. From Hantson et al. (in preparation)

While CO_2 inhibition can explain the spread in different climate scenarios, the calculated trends for the monoterpene emissions is different from isoprene, with a continuous slight decline in monoterpene emissions during the 20th century and first half of the 21st century. This appears surprising taking into account the more or less similar leaf production process of both components (and also the similarities in which emissions are simulated in LPJ-GUESS; [*Arneth et al.*, 2007; *Schurgers et al.*, 2009a]. A large part of this pattern can however be explained by natural changes in vegetation distribution under changing climate. While the normalized emission factors for isoprene are higher in the tropics and decrease towards the poles, the opposite is true for monoterpenes. Therefore a warming climate will lead to a widespread shift in relative abundance of vegetation with higher emissions factors for isoprene and lower emission factors for monoterpenes over most of the globe (e.g. broadleaved trees replacing needle-leaved trees). This shift in relative abundance of PFTs also coincides with the major spatial patterns observed between current and future BVOC emissions, which are especially apparent for the monoterpenes over some temperate regions such as N-America (Figure 5.3.10).

Key message: LPJ-GUESS calculations of BVOC global emissions the RCP4.5 GHG scenario, indicate isoprene emissions increase 41% and monoterpenes 25% in the future compared to current conditions. However, taking the CO_2 inhibition effect into account, emissions decrease slightly with -2% and -13% respectively for isoprene and monoterpenes. Climate change favors isoprene emitting vegetation.

4.2.3 Wildfire emission in Europe

Burned area was calculated with LPJ-GUESS, including SIMFIRE (MOD1; [*Knorr et al.*, 2014]). For this study, simulations were also available with the model LPJmL, with the Spitfire fire routine [*Thonicke et al.*, 2010]. Simulations explored not only effects of climate change but also of different socio-economic pathways, and the associated expectations on human population growth (van Vuuren et al, 2012), which provide a surrogate for effects of land-use change on fire spread and emissions.

The combined effect of climate, atmospheric CO_2 and human population density on future burned area for Europe is shown in Fig. 5.3.12 [*Wu et al.*, 2015]. Both models show a positive trend, leading to a considerable increase in burned area by the end of 21st century. The overall changes in the RCP8.5-SSP5 scenario were around 1.8 (for LPJ-GUESS) and 3.6 (for LPJmL) times the present-day values. Simulations with RCP2.6--SSP1 led to a much more moderate change, with less than 60% increase for both models. Incidentally, the two models differed also with respect to the dominance of woody vs. herbaceous vegetation, the latter being more prominent in LPJ-mL (not shown). The deviation of the burned area between the mean of RCP 8.5 and RCP 2.6 runs became visible in LPJ-GUESS later (around 2040) compared to LPJmL (around 2025).

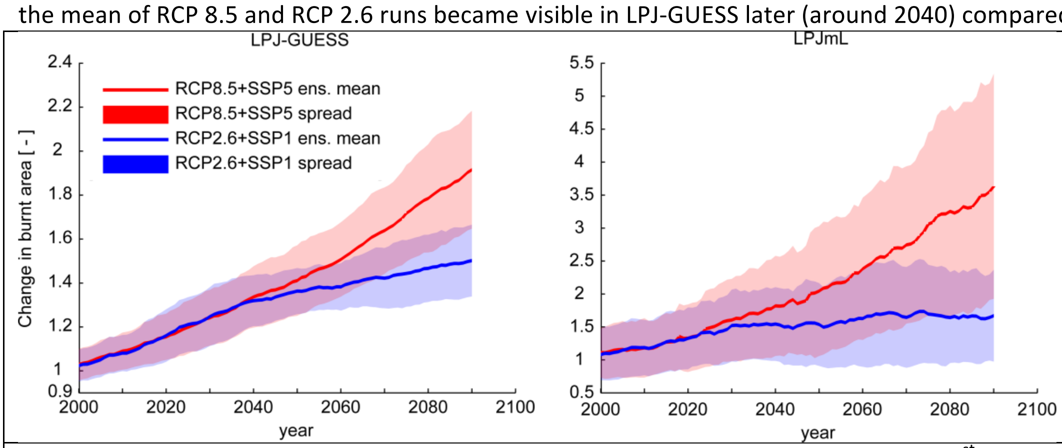

Figure 5.3.12. Simulated relative changes in burned area for Europe to the end of 21st century by two models LPJ-GUESS and LPHmL, represented as ensemble relative change to present-date (1981-2000) for four ESMs for different combinations of climate scenarios RCP 8.5 and RCP 2.6, and socio-economic (SSPs). Spreads are ESMs uncertainties represented as one standard deviation among ESMs from the ensemble mean. All lines are smoothed with 20-year moving average. From Wu et al. (in prep.)

The spatial patterns seen in the RCP8.5-SSP5 and RCP2.6-SSP1 simulations differed in terms of the direction of change in different regions, and also in terms of overall magnitude of change (not shown). Overall, LPJ-GUESS simulated an increase of burned area by 88% and 25% and LPJmL simulated increase by 265% and 34% for Europe for RCP8.5-SSP5 and RCP2.6-SSP1, respectively. Emissions from European forests, using LPJ-GUESS, increase by around 30% from present-day until the end of the 21st century (in the RCP 8.5 climate change scenario; Figure 5.3.13). The increase in emissions is smaller compared to the relative changes in burned area since in the warm, dry RCP8.5 world the biomass production in the model is simulated to decline, which reduces also the available litter for combustion.

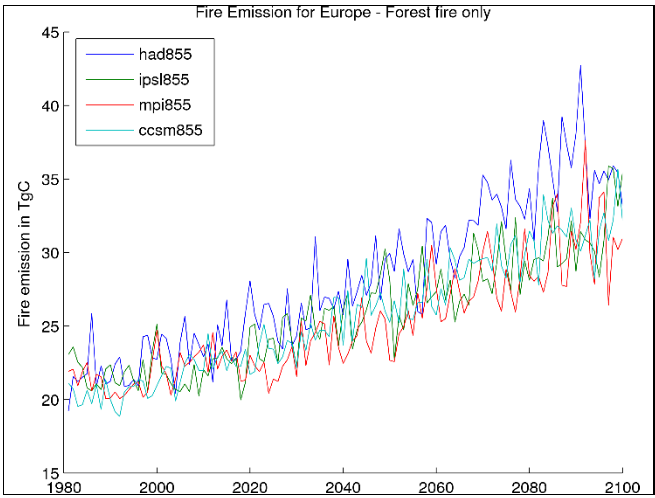

Figure 5.3.13. Simulated total C emissions from forest fires in Europe using LPJ-GUESS and climate change scenarios from four different climate models (for the RCP8.5 emissions scenario. Data from Wu et al [2014].

Key message: Predictions of burnt area in Europe are highly sensitive to the fire module, with increases from the 2000s to the 2100 ranging from 40 % (RCP2.6) and 80 % (RCP8.5) for LPJ-GUESS and 34%-265% for LPJ-Ml. Difference between the distribution of woody and herbaceous vegetation underlie these ranges.
These numbers are associated with an uncertainty of about 50 % associated with the range of climate results from specific climate models. The

4.2.4 Global Wildfire emissions

Globally, the areas with the largest fire risk are located in the tropics, which also dominate today's total wildfire emissions simulated as 1.2 PgC a^{-1}. These totals are on the lower end of typical emission estimates, which is partially because these simulations exclude deforestation fires, and fires in areas dominated by agriculture (Figure 5.3.14, Table 5.3.3)[*Knorr et al.*, 2015].

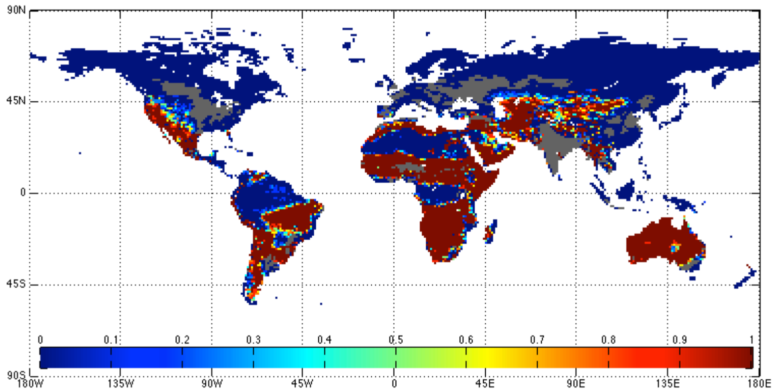

Figure 5.3.14. Fraction of ensemble runs showing grid cell as fire prone (fire frequency >0.01 yr^{-1}) during 1981-2100. From Knorr et al (in preparation). Grey colors denotes regions with >50% agricultural coverage.

In simulations that combine effects of climate change, effects of changing atmospheric CO_2 levels, as well as effects due to socio-economic changes, burned area and wildfire emissions at the end of the 21st century in tropical regions are slightly below present-day levels, and in the extra-tropics slightly above (Figure, table). A number of competing influences are visible in the simulations. First, climate change alone, in a set of factorial experiments, yielded, as expected, globally strongly increasing burned area and emissions (not shown; Knorr et al., in preparation). The effect of enhanced CO_2 levels was more complex: burned area declined (compared to climate-only effects) notably, being at the end of the 21st century around 3.0 (RCP 4.5) and 3.2 (RCP 8.5) Mio km^2 a^{-1}; while climate change effects led to a burned area increase of 3.4 – 4 Mio km^2 a^{-1}. This was largely due to the promotion of woody vegetation growth in savannah areas in response to the CO_2 fertilisation of plants of the C3 photosynthetic type, which reduces fire spread over grass-dominated areas.

The largest effects, however, were seen when population growth, and shifts from rural to urban populations were accounted for. In principle, population growth leads to declining burned area, due to factors ranging from active fire suppression and extinguishing, and enhanced landscape fragmentation preventing fire spread [*Archibald et al.*, 2008; *Knorr et al.*, 2014]. A scenario with relatively high population growth and low degrees of urbanisation (SSP3) thus led to substantially lower burned area and emissions, compared to one with lower population growth and higher urban proportion (SSP1; table 5.3.3)

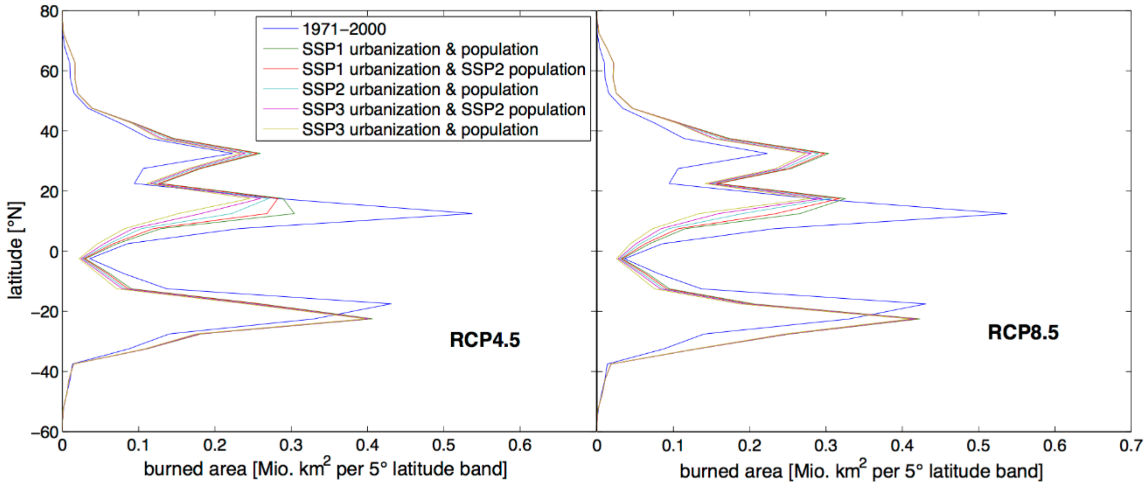

Figure 5.3.15: Ensemble average of simulated burned area by latitude for current climate (1971-2000) and for 2071-2100 for different SSP demography scenarios. Left: emissions associated with RCP4.5 climate, right: RCP8.5 climate. From Knorr et al. (in preparation).

Table 5.3.3*: Ensemble averages of simulated wildfire emissions by scenario for late 20th and 21st century. Numbers shown combine climate change, CO2 and population effects.*

	RCP	Population	Urbanization	Tropics	Extra-tropics
1971-2000	-	Historical	Historical	0.608	0.538
2071-2100	4.5	SSP1	SSP1	0.513	0.672
	4.5	SSP3	SSP3	0.387	0.642
2071-2100	8.5	SSP1	SSP1	0.522	0.776
	8.5	SSP3	SSP3	0.396	0.740

Key Message: LPJ-GUESS calculations of wildfire emissions indicate a complex range of interactions between vegetation, climate change and increasing CO2, and fire suppression. Comparing 1970-2000 and 2070-2100, overall tropical emissions decline between 15 and 35 % (mostly due human influence), while extratropical emissions increase by 20 % and 45 %. Globally emissions change within a -10 % range.

4.2.5 Effects of Nitrogen deposition on ecosystem processes in Europe

Preliminary model simulations were performed to investigate the effects of N deposition and fertilisation on various ecosystem properties, such as carbon pools and carbon fluxes. Table 5.3.4 indicates that accounting for real historical land cover changes, i.e. conversion of natural vegetation into croplands, (“crop”) over simulations with potential natural vegetation cover (“pnv”) reduces both total carbon pools in ecosystems, as well as annual exchange of CO_2 with the atmosphere. When accounting for N input and land use change, NPP overall was larger compared to the C-only version of the model, however total C-pools in ecosystems were reduced.

	C pool		NPP		NEE	
simulation	1961—1990	1996—2005	1961—1990	1996—2005	1961—1990	1996—2005
crop C	243,65	247,07	-4,73	-4,73	-0,08	-0,18
crop C-N	176,76	179,48	-6,51	-6,61	-0,11	-0,07
PNV	306,12	312,81	-5,20	-5,54	-0,22	-0,30

Table 5.3.4: Simulated C pools, net primary productivity (NPP) and net ecosystem carbon exchange (NEE) in Europe (30-75°N and 20°W - 45°E) for two historical time periods. The numbers shown are for potential natural vegetation (PNV), and considering real land cover (Crop), with the carbon-only version, and the CN-version of the model. Numbers are in PgC (pools) and PgC a^{-1} (fluxes).

These simulations are currently investigated further, and simulations also planned over the coming months, as part of Eclaire, to study effects of N-input on yields as well as N leaching from ecosystems.

4.2.6 Global Effects of Nitrogen deposition on ecosystem processes

In LPJ-GUESS, accounting for carbon-nitrogen coupling in ecosystems has been shown to lead CO_2–fertilisation response of boreal ecosystems, that is more in line with free-air carbon enrichment studies [*Smith et al.*, 2014]. On global scale level, accounting for N constraints on carbon uptake and storage in terrestrial ecosystems fits also better with stoichiometric estimates of carbon budget constraints (compared to the C-only version of the model) [*Hungate et al.*, 2003; *Smith et al.*, 2014]. Global net primary productivity in the C-only version of the model was simulated as 61 PgC a^{-1} averaged over the period 1961-1990, compared to 58 PgC a^{-1} in the CN version. In future, effects of atmospheric CO_2 concentration and climate change on net terrestrial carbon uptake greatly outweighed that of nitrogen deposition.Likewise, response to historical N-deposition on natural ecosystems has been small [*Wårlind et al.*, 2014], the direct effect of N deposition to global ecosystems, with respect to the changes in carbon sink strength are negligible (see *Wårlind et al.*, 2014, and references therein). However, N deposition has large effects on two contrasting processes that are of large importance for CO_2 removal from the atmosphere. On the one hand, nitrogen limitation dampens the stimulating effect of CO_2- fertilisation on plant photosynthesis and carbon storage in vegetation. On the other hand, climate change enhances N mineralisation in (the warmer) soils, which makes relatively more N available for plant growth (Arneth, et al 2010). The net effects on terrestrial C uptake and vegetation growth have been shown to be small; in LPJ-GUESS, accounting for N input even (slightly) enhances the future C sink strength [*Wårlind et al.*, 2014]. This contrast the net effects of other model experiments that compared C-only and CN versions of models in which a more or less pronounced decline of cumulative 21st carbon uptake in the CN versions was observed (see summary in [*Wårlind et al.*, 2014]). One possibly reason for this slightly diverging result might recide with complex interactions with vegetation distribution. But it also highlights how, considering uncertainty in existing models, small difference between two relatively large opposing factors (CO_2 vs. climate impacts on C-cycle) can lead to pronounced effects on calculated carbon net-exchanges.

Key-message: While nitrogen input to ecosystems affects yields and can lead to pollution of watersheds in heavily fertilised regions, effects of N deposition on natural ecosystems regarding the historical carbon sink strength are minor. Whether or not nitrogen limitation of plant growth will notably affect future ecosystem carbon storage is under debate, and current modelling studies show conflicting results. Arguably, climate effects of N_2O emissions are of more concern than N-interactions with the C sink; this will be investigated further in the coming years with updated versions of LPJ-GUESS

5. Milestones achieved:

Evaluation of AR5 and other simulations with climate and chemistry global models (month 18) were fully achieved in Month 24.

6. Deviations and reasons:

D5.3 was delivered with a delay of about three months. These minor delays were due to earlier delays in D5.1 and D5.4.

7. Publications:

Hantson, S., W. Knorr, T. A. M. Pugh, G. Schurgers, and A. Arneth (2015), Effects of land-cover change on future BVOC emissions, *in prep..*

Knorr, W., A. Arneth, and L. Jian (2015), Demographic controls of future fire risks, *in prep.*

Rosenkranz, M., T. A. M. Pugh, J.-P. Schnitzler, and A. Arneth (2014), Effect of land-use change and management on BVOC emissions – selecting climate-smart cultivars, *Plant, Cell, and Environment*, in press.

Wu, M., W. Knorr, K. Thonicke, G. Schurgers, and A. Arneth (2015), Uncertainties in the impacts of climate change, atmospheric CO2 levels and demography on future burned area in Europe: comparison between two fire-vegetation models, *in prep. will have Eclaire ackn*

Other references:

Ahlstrom, A., G. Schurgers, A. Arneth, and B. Smith (2012), Robustness and uncertainty in terrestrial ecosystem carbon response to CMIP5 climate change projections, *Environmental Research Letters*, *7*(4).

Andreae, M. O., and P. Merlet (2001), Emission of trace gases and aerosols from biomass burning, *Global Biogeochemical Cycles*, *15*(4), 955-966.

Archibald, S., D. P. Roy, B. W. van Wilgen, and R. J. Scholes (2008), What limits fire?: An examination of drivers of burnt area in Southern Africa, *Global Change Biology*, doi: 10.1111/j.1365-2486.2008.01754.x.

Arneth, A., G. Schurgers, T. Hickler, and P. A. Miller (2008a), Effects of species composition, land surface cover, CO_2 concentration and climate on isoprene emissions from European forests, *Plant Biology*, *10*(1), 150-162, doi:110.1055/s-2007-965247.

Arneth, A., R. K. Monson, G. Schurgers, U. Niinemets, and P. I. Palmer (2008b), Why are estimates of global terrestrial isoprene emissions so similar (and why is this not so for monoterpenes)?, *Atmospheric Chemistry and Physics*, *8*(16), 4605-4620.

Arneth, A., et al. (2010), Terrestrial biogeochemical feedbacks in the climate system, *Nature Geoscience*, *3*(8), 525-532.

Arneth, A., G. Schurgers, J. Lathiere, T. Duhl, D. J. Beerling, C. N. Hewitt, M. Martin, and A. Guenther (2011), Global terrestrial isoprene emission models: sensitivity to variability in climate and vegetation, *Atmospheric Chemistry and Physics*, *11*(15), 8037-8052.

Arneth, A., Harrison, S. P., Zaehle, S., Tsigaridis, K., Menon, S., Bartlein, P. J., Feichter, J., Korhola, A., Kulmala, M., O'Donnell, D., Schurgers, G., Sorvari, S., and Vesala, T.: Terrestrial biogeochemical feedbacks in the climate system, Nature Geoscience, 3, 525-532, 10.1038/ngeo905, 2010.

Arneth, A., et al. (2007), Process-based estimates of terrestrial ecosystem isoprene emissions: incorporating the effects of a direct CO_2-isoprene interaction, *Atmospheric Chemistry and Physics*, *7*, 31-53.

Fang H., Wei S., Jiang C., Scipal K., Theoretical uncertainty analysis of global MODIS, CYCLOPES, and GLOBCARBON LAI products using a triple collocation method. Remote Sensing of Environment, Volume 124, September 2012, Pages 610-621, ISSN 0034-4257.

Fang, H., et al. (2013), Characterization and intercomparison of global moderate resolution leaf area index (LAI) products: Analysis of climatologies and theoretical uncertainties, J. Geophys. Res. Biogeosci., 118, 529–548, doi:10.1002/jgrg.20051.

Garrigues, S., et al. (2008), Validation and intercomparison of global Leaf Area Index products derived from remote sensing data, J. Geophys. Res., 113, G02028, doi:10.1029/2007JG000635.

Guenther, A. B., Jiang, X., Heald, C. L., Sakulyanontvittaya, T., Duhl, T., Emmons, L. K., and Wang, X.: The Model of Emissions of Gases and Aerosols from Nature version 2.1 (MEGAN2.1): an extended and updated framework for modeling biogenic emissions, Geosci. Model Dev., 5, 1471-1492, doi:10.5194/gmd-5-1471-2012, 2012.

Hungate, B. A., J. S. Dukes, M. R. Shaw, Y. Q. Luo, and C. B. Field (2003), Nitrogen and climate change, *Science*, *302*(5650), 1512-1513.

Kjellström, E., Nikulin, G., Hansson, U., Strandberg, G., & Ullerstig, A. (2011). 21st century changes in the European climate: uncertainties derived from an ensemble of regional climate model simulations. Tellus A, 63(1), 24-40.

Lathière, J., Hauglustaine, D. A., Friend, A., De Noblet-Ducoudré, N., Viovy, N., and Folberth, G.: Impact of climate variability and land use changes on global biogenic volatile organic compound emissions, Atmos. Chem. Phys., 6, 2199–2146, 2006.

Kesselmeier, J., and M. Staudt (1999), Biogenic volatile organic compounds (VOC): An overview on emission, physiology and ecology, *Journal of Atmospheric Chemistry*, *33*, 23-88.

Knorr, W., V. Lehsten, and A. Arneth (2012), Determinants and predictability of global wildfire emissions, *Atmospheric Chemistry and Physics*, *12*(15), 6845-6861.

Knorr, W., T. Kaminski, A. Arneth, and U. Weber (2014), Impact of human population density on fire frequency at the global scale, *Biogeosciences*, *11*(4), 1085-1102.

Lindeskog, M., A. Arneth, A. Bondeau, K. Waha, J. Seaquist, S. Olin, and B. Smith (2013), Implications of accounting for land use in simulations of ecosystem carbon cycling in Africa, *Earth System Dynamics*, *4*(2), 385-407.

Niinemets, U., R. K. Monson, A. Arneth, P. Ciccioli, J. Kesselmeier, U. Kuhn, S. M. Noe, J. Penuelas, and M. Staudt (2010), The leaf-level emission factor of volatile isoprenoids: caveats, model algorithms, response shapes and scaling, *Biogeosciences*, *7*(6), 1809-1832.

Possell M, Hewitt CN, Beerling DJ (2005) The effects of glacial atmospheric CO2 concentrations and climate on isoprene emissions by vascular plants. Global Change Biology, 11, 60–69.

Schurgers, G., A. Arneth, R. Holzinger, and A. H. Goldstein (2009a), Process-based modelling of biogenic monoterpene emissions combining production and release from storage, *Atmospheric Chemistry and Physics*, *9*(10), 3409-3423.

Schurgers, G., T. Hickler, P. A. Miller, and A. Arneth (2009b), European emissions of isoprene and monoterpenes from the Last Glacial Maximum to present, *Biogeosciences*, *6*(12), 2779-2797.

Sindelarova, K., C. Granier, I. Bouarar, A.B. Guenther, S. Tilmes, T. Stavrakou, J.-F. Müller, U. Kuhn, P. Stefani, and W. Knorr, 2014: Global data set of biogenic VOC emissions calculated by the MEGAN model over the last 30 years. Atmospheric Chemistry and Physics, 14, 9317-9341, DOI: 10.5194/acp-14-9317-2014.

Smith, B., I. C. Prentice, and M. T. Sykes (2001), Representation of vegetation dynamics in the modelling of terrestrial ecosystems: comparing two contrasting approaches within European climate space, *Global Ecology & Biogeography*, *10*, 621-637.

Smith, B., D. Warlind, A. Arneth, T. Hickler, P. Leadley, J. Siltberg, and S. Zaehle (2014), Implications of incorporating N cycling and N limitations on primary production in an individual-based dynamic vegetation model, *Biogeosciences*, *11*(7), 2027-2054.

Spitters, C.J.T., Toussaint, H.A.J.M. and Goudriaan, J., 1986. Separating the diffuse and direct component of global radiation and its implications for modeling canopy photosynthesis. Part I. Components of incoming radiation. Agric. For. Meteorol., 38: 217-229.

Spitters, C.J.T, 1986. Separating the diffuse and direct component of global radiation and its implications for modeling canopy photosynthesis. Part II. Calculation of canopy photosynthesis. Agric. For. Meteorol., 38: 231-242.

Thonicke, K., A. Spessa, I. C. Prentice, S. P. Harrison, L. Dong, and C. Carmona-Moreno (2010), The influence of vegetation, fire spread and fire behaviour on global biomass burning and trace gas emissions, *Biogeosciences*, *7*(6), 1991-2011.

Wårlind, D., B. Smith, T. Hickler, and A. Arneth (2014), Nitrogen feedbacks increase future terrestrial ecosystem carbon uptake in an individual-based dynamic vegetation model, *Biogeosciences*, *11*(21), 6131-6146.

van Vuuren, D. P., Riahi, K., Moss, R., Edmonds, J., Thomson, A., Nakicenovic, N., Kram, T., Berkhout, F., Swart, R., Janetos, A., Rose, S. K., and Arnell, N.: A proposal for a new scenario framework to support research and assessment in different climate research communities, Global Environmental Change, 22, 21-35, 10.1016/j.gloenvcha.2011.08.002, 2012.

Wilkinson, M. J., Monson, R. K., Trahan, N., Lee, S., Brown, E., Jackson, R. B., Polley, H. W.,Fay P. A., Fall, R. (2009). Leaf isoprene emission rate as a function of atmospheric CO2 concentration. Global Change Biology, 15(5), 1189-1200.

Yuan, H., Dai, Y., Xiao, Z., Ji, D., and Shangguan, W.: Reprocessing the MODIS Leaf Area Index products for land surface and climate modelling, Remote Sens. Environ., 115, 1171–1187, 2011.

8. Meetings:

Participation in ECLAIRE plenary meetings.

9. List of Documents/Annexes:

None.